

## Superconducting Transition Temperatures of up to 47 K from Simultaneous Rare-Earth Element and Antimony Doping of 112-Type $\text{CaFeAs}_2$

Kazutaka Kudo<sup>1,2\*</sup>, Yutaka Kitahama<sup>1</sup>, Kazunori Fujimura<sup>1</sup>,  
Tasuku Mizukami<sup>1</sup>, Hiromi Ota<sup>3</sup>, and Minoru Nohara<sup>1,2†</sup>

<sup>1</sup>Department of Physics, Okayama University, Okayama 700-8530, Japan

<sup>2</sup>Research Center of New Functional Materials for Energy Production, Storage and Transport, Okayama University, Okayama 700-8530, Japan

<sup>3</sup>Division of Instrumental Analysis, Department of Instrumental Analysis & Cryogenics, Advanced Science Research Center, Okayama University, Okayama 700-8530, Japan

The effects of simultaneous Sb doping on the superconductivity of 112-type  $\text{Ca}_{1-x}\text{RE}_x\text{FeAs}_2$  ( $\text{RE} = \text{La}, \text{Ce}, \text{Pr}, \text{and Nd}$ ) were studied through measurements of the magnetization and electrical resistivity. In Sb-free materials, the superconducting transition temperature  $T_c$  of the La-doped sample was 35 K, while those of the Pr- and Nd-doped samples were  $\sim 10$  K; no superconductivity was observed in the Ce-doped sample. Sb doping increased the  $T_c$  of all RE-doped samples:  $T_c$  increased to 47, 43, 43, and 43 K for  $\text{RE} = \text{La}, \text{Ce}, \text{Pr}, \text{and Nd}$ , respectively. We also found that the enhanced superconductivity results from the increase in the lattice parameter  $b$ , which increases the As-Fe-As bond angle to be closer to the ideal tetrahedron value. These observations provide insight for further increasing the  $T_c$  of the 112 phase.

The discovery of iron-based superconductors has stimulated the development of novel superconducting materials<sup>1–3</sup> such as  $\text{REFeAsO}$  (1111 type),<sup>4</sup>  $\text{AEFe}_2\text{As}_2$  (122 type),<sup>5,6</sup>  $\text{AFeAs}$  (111 type),<sup>7</sup> and  $\text{FeSe}$  (11 type)<sup>8</sup> that contain rare-earth (RE), alkali-earth (AE), and alkali (A) elements, as well as the development of compounds with perovskite- and/or rocksalt-type<sup>9–12</sup> and pyrite-type spacer layers.<sup>13–18</sup> For this class of materials, the maximum superconducting transition temperature  $T_c$  is 55 K,<sup>19</sup> and new iron-based superconducting materials will need to be developed to further increase  $T_c$ .

To this end, novel 112-type iron arsenides of  $\text{Ca}_{1-x}\text{La}_x\text{FeAs}_2$ ,  $\text{Ca}_{1-x}\text{Pr}_x\text{FeAs}_2$ , and  $\text{Ca}_{1-x}\text{RE}_x\text{FeAs}_2$  ( $\text{RE} = \text{Ce}, \text{Nd}, \text{Sm}, \text{Eu}, \text{and Gd}$ ) reported by Katayama *et al.*,<sup>20</sup> Yakita *et al.*,<sup>21</sup> and Sala *et al.*,<sup>22</sup> respectively, have received considerable attention, and it has been recognized that the RE substitution is necessary for stabilizing the 112 phase.<sup>20–22</sup> These compounds crystallize in a monoclinic structure with a space group of  $P2_1$  (No. 4)<sup>20</sup> or  $P2_1/m$  (No. 11)<sup>21,22</sup> and consist of alternately stacked FeAs and arsenic zigzag bond layers, which are a notable feature. The arsenic zigzag bond layers are considered to be composed of  $\text{As}^-$  ions with a  $4p^4$  configuration as found in  $\text{REAs}_2$  ( $T = \text{Ag}, \text{Au}$ ).<sup>23</sup> Thus, the chemical formula for these compounds can be written as  $(\text{Ca}_{1-x}^{2+}\text{RE}_x^{3+})(\text{Fe}^{2+}\text{As}^{3-})\text{As}^- \cdot xe^-$  with an excess charge of  $xe^-/\text{Fe}$  injected into the  $\text{Fe}^{2+}\text{As}^{3-}$  layers. Most 112-type iron arsenides exhibit superconductivity: La-doped compounds show bulk superconductivity at 35 K,<sup>24</sup> while Pr-, Nd-, Sm-, Eu-, and Gd-doped compounds show superconductivity at 10–15 K with a small shielding volume fraction (VF) of 5–20%.<sup>21,22</sup> Ce-doped compounds rarely

exhibit superconductivity.<sup>22</sup>

Recently, it was reported that the simultaneous doping of isovalent P or Sb drastically improves the superconductivity in the La-doped 112 phase;  $T_c$  increased to 41 and 43 K as a result of 0.5% P and 1% Sb doping, respectively.<sup>24</sup> In this Letter, we report that a large amount of Sb doping further increases the  $T_c$  of  $\text{Ca}_{1-x}\text{La}_x\text{Fe}(\text{As}_{1-y}\text{Sb}_y)_2$  to 47 K, which is the second highest  $T_c$  after 1111-type iron-based superconductors. Moreover, we show that bulk superconductivity at 43, 43, and 43 K is induced by the simultaneous Sb doping of  $\text{Ca}_{1-x}\text{RE}_x\text{FeAs}_2$  with  $\text{RE} = \text{Ce}, \text{Pr}, \text{and Nd}$ , respectively, and that an increase in the lattice parameter  $b$ , which modifies the As-Fe-As bond angle, is important for optimizing the superconductivity in the 112 phase.

Single crystals of  $\text{Ca}_{1-x}\text{RE}_x\text{Fe}(\text{As}_{1-y}\text{Sb}_y)_2$  ( $\text{RE} = \text{La}, \text{Ce}, \text{Pr}, \text{and Nd}$ ) were grown by heating a mixture of Ca, RE, FeAs, As, and Sb powders with nominal compositions of  $x = 0.10$  and  $0.00 \leq y \leq 0.10$  (grown quantities of the 112 phase drastically decrease for  $y \geq 0.20$ ). A stoichiometric amount of the mixture was then placed in an aluminum crucible and sealed in an evacuated quartz tube. Samples were prepared in a globe box filled with argon gas. The ampules were heated at 700 °C for 3 h, heated to 1100 °C at a rate of 46 °C/h, and then cooled to 1050 °C at a rate of 1.25 °C/h before furnace cooling. The obtained samples were characterized by powder X-ray diffraction (XRD) using a Rigaku RINT-TTR III X-ray diffractometer with  $\text{CuK}\alpha$  radiation and by single-crystal XRD using a Rigaku Single Crystal X-ray Structural Analyzer (Varimax with Saturn).  $\text{Ca}_{1-x}\text{RE}_x\text{Fe}(\text{As}_{1-y}\text{Sb}_y)_2$  samples were obtained together with a powder mixture of REAs, FeAs,  $\text{FeAs}_2$ , and  $\text{CaFe}_2\text{As}_2$ . The single crystals of  $\text{Ca}_{1-x}\text{RE}_x\text{Fe}(\text{As}_{1-y}\text{Sb}_y)_2$  separated from the

\*kudo@science.okayama-u.ac.jp

†nohara@science.okayama-u.ac.jp

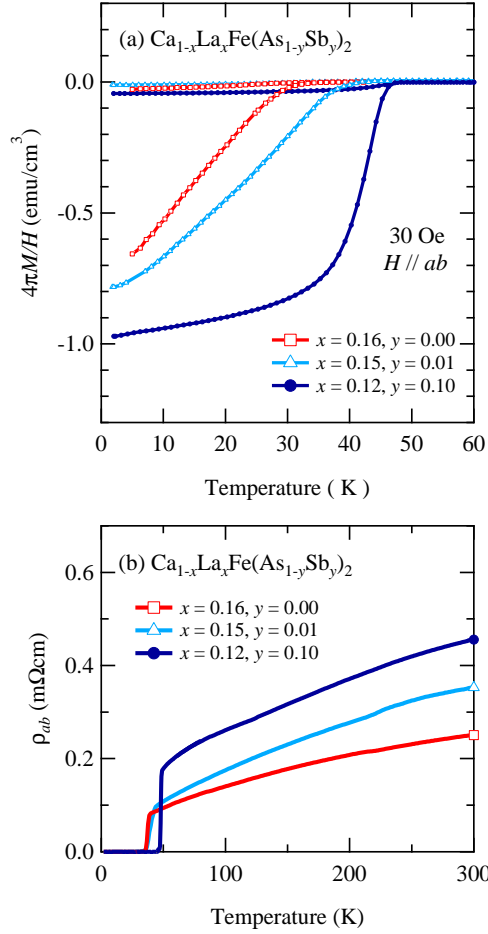


**Fig. 1.** (Color online) (a) Temperature dependence of the magnetization  $M$  of  $\text{Ca}_{1-x}\text{La}_x\text{Fe}(\text{As}_{1-y}\text{Sb}_y)_2$  measured at a magnetic field  $H$  of 30 Oe parallel to the  $ab$  plane under zero-field-cooling and field-cooling conditions. (b) Temperature dependence of the electrical resistivity  $\rho_{ab}$  of  $\text{Ca}_{1-x}\text{La}_x\text{Fe}(\text{As}_{1-y}\text{Sb}_y)_2$  parallel to the  $ab$  plane.

mixture were plate-like with typical dimensions of  $(0.3\text{--}0.7) \times (0.3\text{--}0.7) \times 0.02 \text{ mm}^3$ .

The  $RE$  content  $x$  was analyzed by energy-dispersive X-ray spectrometry (EDS), but the Sb content  $y$  could not be determined by EDS because the Sb peak positions in the EDS spectra overlapped those of Ca. We thus assumed a nominal  $y$ . Although the nominal  $x$  was fixed at 0.1, the  $x$  values measured by EDS varied with the nominal  $y$ . For example,  $\text{Ca}_{1-x}\text{La}_x\text{Fe}(\text{As}_{1-y}\text{Sb}_y)_2$  had compositions of  $x = 0.16, 0.15$ , and  $0.12$  with nominal  $y = 0.00, 0.01$ , and  $0.10$ , respectively; i.e., the La content tended to decrease with increasing  $y$ . In contrast, for  $\text{Ca}_{1-x}\text{La}_x\text{Fe}(\text{As}_{1-y}\text{Sb}_y)_2$  ( $RE = \text{Ce}, \text{Pr}, \text{and Nd}$ ), we found compositions of  $x = 0.15\text{--}0.25$  with nominal  $y = 0.00, 0.01, 0.05$ , and  $0.10$ ; there was no clear relation between  $x$  and  $y$ .

The magnetization  $M$  in a magnetic field of 30 Oe parallel to the  $ab$  plane was measured using a Quantum Design magnetic property measurement system (MPMS). The  $T_c$  values

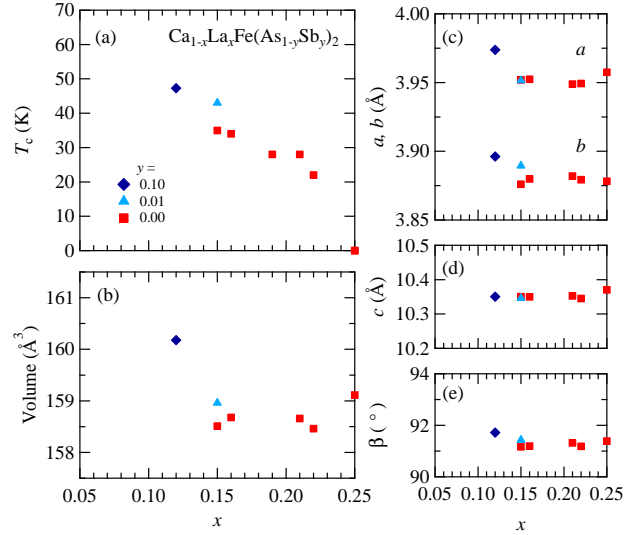


**Fig. 2.** (Color online) Dependence of the (a)  $T_c$ , (b) cell volume, (c)  $a$  and  $b$  parameters, (d)  $c$  parameter, and (e)  $\beta$  angle of  $\text{Ca}_{1-x}\text{La}_x\text{Fe}(\text{As}_{1-y}\text{Sb}_y)_2$  on  $x$ .

were determined from the onset of the diamagnetism, which is characteristic of the superconducting transition. Electrical resistivity  $\rho_{ab}$  parallel to the  $ab$  plane was also measured using a standard DC four-terminal method in a Quantum Design physical property measurement system (PPMS).

The enhancement in the superconductivity of the Sb-doped  $\text{Ca}_{1-x}\text{La}_x\text{FeAs}_2$  can be observed in the temperature dependence of  $M$  shown in Fig. 1(a). Previous studies<sup>20,24</sup> have reported that La-doped samples with  $y = 0.00$  show diamagnetic behavior below  $T_c = 34$  K, and  $T_c$  increased to 43 K for  $y = 0.01$ .<sup>24</sup> The values of VF at the lowest temperature were previously estimated to be 66% and 78% for  $y = 0.00$ <sup>20</sup> and  $0.01$ ,<sup>24</sup> respectively, indicating bulk superconductivity. We found that a large amount of Sb doping leads to a further increase in  $T_c$  to 47 K. As shown in Fig. 1(a), the La-doped sample with  $y = 0.10$  exhibits clear diamagnetic behavior below  $T_c = 47$  K, and the VF at 2 K was estimated to be approximately 100%, which supports the emergence of bulk superconductivity. Further evidence of the enhanced superconductivity was obtained from the temperature dependence of  $\rho_{ab}$ , as shown in Fig. 1(b). We found that  $\rho_{ab}$  for the La-doped  $y = 0.10$  sample exhibited a sharp drop below 49 K, and zero resistivity was observed at 47 K; both these temperatures are much higher than those of the  $y = 0.00$ <sup>20</sup> and  $0.01$ <sup>24</sup> samples.

The increased  $T_c$  of  $\text{Ca}_{1-x}\text{La}_x\text{Fe}(\text{As}_{1-y}\text{Sb}_y)_2$  can be explained by two effects originating from the simultaneous Sb doping: a decrease in the La content and an increase in the cell volume. In  $\text{Ca}_{1-x}\text{La}_x\text{FeAs}_2$ , it is known that  $T_c$  increases with decreasing  $x$  and exhibits a maximum value of 35 K at the lowest  $x$  of 0.15,<sup>24</sup> as shown in Fig. 2(a); a sample with a lower  $x$  could potentially have a higher  $T_c$ . Simultaneous Sb

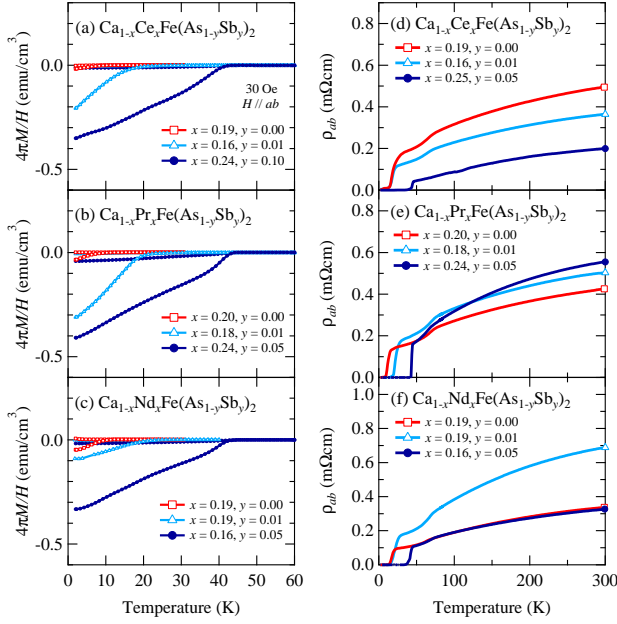


**Fig. 3.** (Color online) (a)(b)(c) Temperature dependence of the magnetization  $M$  of  $\text{Ca}_{1-x}\text{RE}_x\text{Fe}(\text{As}_{1-y}\text{Sb}_y)_2$  ( $\text{RE} = \text{Ce}, \text{Pr}, \text{and Nd}$ ) measured at a magnetic field  $H$  of 30 Oe parallel to the  $ab$  plane under zero-field-cooling and field-cooling conditions. (d)(e)(f) Temperature dependence of the electrical resistivity  $\rho_{ab}$  of  $\text{Ca}_{1-x}\text{RE}_x\text{Fe}(\text{As}_{1-y}\text{Sb}_y)_2$  ( $\text{RE} = \text{Ce}, \text{Pr}, \text{and Nd}$ ) parallel to the  $ab$  plane.

doping allows the La content to be reduced to  $x = 0.12$ , and as expected,  $T_c$  increased to 47 K. In general, chemical substitution modifies the number of charge carriers and induces a chemical pressure. The primal role of La doping is charge carrier modification because the cell volume [Fig. 2(b)] and lattice parameters<sup>24</sup> [Figs. 2(c), (d), and (e)] of  $\text{Ca}_{1-x}\text{La}_x\text{FeAs}_2$  exhibit no significant changes upon La doping owing to the similar ionic radii of  $\text{Ca}^{2+}$  and  $\text{La}^{3+}$ . Thus, a decrease in the La content corresponds to a reduction in the number of charge carriers. Secondly, simultaneous Sb doping applies a negative chemical pressure that increases the cell volume, as shown in Fig. 2(b), because the ionic radius of  $\text{Sb}^{3-}$  ( $\text{Sb}^-$ ) is larger than that of  $\text{As}^{3-}$  ( $\text{As}^-$ ). The increased cell volume is a result of an increase in the in-plane lattice parameters  $a$  and  $b$ , as shown in Fig. 2(c); in contrast, the  $c$  parameter hardly changes, as shown in Fig. 2(d). In iron-based superconductors, the expansion can effectively optimize the superconductivity, which is sensitive to modifications in the crystal structure.<sup>25–28</sup> Note that the enhancement of  $T_c$  by 0.5% P doping in the La-doped system, which was reported in our previous article,<sup>24</sup> should be attributed to a different mechanism because the small amount of P doping<sup>29</sup> neither reduced the La content nor changed the lattice parameters.<sup>24</sup> However, the exact mechanism is still unclear.

A similar enhancement in the superconductivity was also observed in Sb-doped  $\text{Ca}_{1-x}\text{RE}_x\text{FeAs}_2$  ( $\text{RE} = \text{Ce}, \text{Pr}, \text{and Nd}$ ). As shown in Figs. 3(a), (b), and (c), in the Sb-free samples,

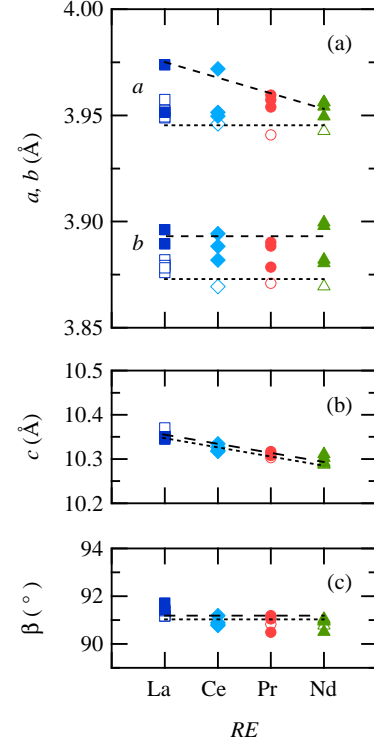


**Fig. 4.** (Color online) Dependences of the (a)  $a$  and  $b$  parameters, (b)  $c$  parameter, and (c)  $\beta$  angle of  $\text{Ca}_{1-x}\text{RE}_x\text{Fe}(\text{As}_{1-y}\text{Sb}_y)_2$  ( $\text{RE} = \text{La}, \text{Ce}, \text{Pr}, \text{and Nd}$ ) on  $\text{RE}$ . The open and closed symbols indicate the lattice parameters of Sb-free samples and Sb-doped samples, respectively. The dotted and broken lines are, respectively, guides to the eye for the lattice parameters of Sb-free samples and Sb-doped samples with the highest  $T_c$  for each  $\text{RE}$ -doped systems.

the Ce-doped system shows no bulk superconductivity down to 2 K, while the Pr- and Nd-doped systems exhibit superconductivity at 10 and 11 K, respectively, with a small VF of 5%. These results are consistent with previous reports.<sup>21,22</sup> Sb doping resulted in higher  $T_c$  values of 21 and 43 K in Ce-doped systems of  $y = 0.01$  and 0.10, respectively, 26 and 43 K in Pr-doped systems of  $y = 0.01$  and 0.05, respectively, and 24 and 43 K in Nd-doped systems of  $y = 0.01$  and 0.05, respectively. Thus, we found that Sb-doped 112 phase samples have a  $T_c$  of higher than 40 K irrespective of  $\text{RE}$ . More importantly, Sb substitution resulted in a substantial increase in the VF, indicating the emergence of bulk superconductivity. Evidence of the enhanced superconductivity was also found in the temperature dependence of  $\rho_{ab}$ . As shown in Figs. 3(d), (e), and (f),  $\rho_{ab}$  of  $\text{Ca}_{1-x}\text{RE}_x\text{Fe}(\text{As}_{1-y}\text{Sb}_y)_2$  ( $\text{RE} = \text{Ce}, \text{Pr}, \text{and Nd}$ ) with  $y = 0.05$  was zero at 37, 43, and 37 K, respectively; these temperatures are much higher than those (5, 9, and 13 K) of the Sb-free samples. Note that the zero resistivity observed in the Sb-free  $\text{Ca}_{1-x}\text{Ce}_x\text{FeAs}_2$  sample is attributed to filamentary superconductivity because there is no visible diamagnetic signal at  $T_c$ . In  $\text{Ca}_{1-x}\text{RE}_x\text{Fe}(\text{As}_{1-y}\text{Sb}_y)_2$  ( $\text{RE} = \text{Ce},$

Pr, and Nd), while we have observed the importance of the volume effect [Figs. 4(a) and (b)] in the enhanced superconductivity in the same manner as discussed for the La-doped system, the precise  $x$  and  $y$  dependences of the  $T_c$  are still unclear.

On considering the well-known relation between  $T_c$  and local structure in the iron-based superconductors,<sup>25–28</sup> the most important factor that determines the volume effect, which enhances superconductivity, is the increase in the  $b$  parameter. In general, iron-based superconductors with high  $T_c$ , such as 1111-type superconductors with  $T_c > 50$  K, satisfy the following structural conditions: the Fe and As atoms form an ideal tetrahedral structure (i.e., the As-Fe-As bond angle  $\alpha = 109.47^\circ$ )<sup>25,26</sup> and the As height with respect to the Fe plane,  $h_{Pn}$ , is approximately 1.38 Å.<sup>27,28</sup> Because of the monoclinic structure, the 112 phase possesses two bond angles:  $\alpha_a$  and  $\alpha_b$ , which correspond to the  $\alpha$ -angle along the  $a$  and  $b$  axes, respectively. Our preliminary structural analysis<sup>30</sup> of  $\text{Ca}_{1-x}\text{La}_x\text{Fe}(\text{As}_{1-y}\text{Sb}_y)_2$  with  $T_c = 47$  K showed that  $\alpha_b$  is drastically improved by Sb doping:  $\alpha_a = 109.098^\circ$  and  $\alpha_b = 107.061^\circ$  in the Sb-free sample,<sup>20</sup> while  $\alpha_a = 109.731^\circ$  and  $\alpha_b = 108.655^\circ$  in the Sb-doped sample. The result suggests that the increase in  $b$  parameter [Fig. 4(a)], which increases  $\alpha_b$ , is a key factor for enhancing the superconductivity in the 112 phase.<sup>31</sup> On the other hand, Sb doping does not modify  $h_{Pn}$  as much, because the  $c$  parameter is almost insensitive to Sb doping [Fig. 4(b)]. In both Sb-free and Sb-doped samples, the  $h_{Pn}$  values are slightly larger than the ideal value:  $h_{Pn} = 1.418$  and 1.408 Å in the Sb-free<sup>20</sup> and Sb-doped samples, respectively. We expect that the  $T_c$  of the 112 phase can be increased above 50 K, if the  $b$  parameter can be increased to approximately equal  $a$  and, simultaneously, the  $c$  parameter can be slightly decreased.

In summary, the effects of Sb doping on the  $T_c$  of 112-type  $\text{Ca}_{1-x}\text{RE}_x\text{FeAs}_2$  ( $\text{RE} = \text{La}, \text{Ce}, \text{Pr}, \text{and Nd}$ ) were studied through measurements of the magnetization and electrical resistivity. Sb-doping results in an increase in  $T_c$  such that the  $T_c$  values of Sb-doped  $\text{Ca}_{1-x}\text{RE}_x\text{FeAs}_2$  with  $\text{RE} = \text{La}, \text{Ce}, \text{Pr}, \text{and Nd}$  were 47, 43, 43, and 43 K, respectively. We found that an increase in the  $b$  parameter, which improves the As-Fe-As bond angle, is important for enhancing the superconductivity in the 112 phase.

**Acknowledgments** This work was partially supported by Grants-in-Aid for Scientific Research (B) (26287082) and (C) (25400372) from the Japan Society for the Promotion of Science (JSPS) and the Funding Program for World-Leading Innovative R&D on Science and Technology (FIRST Program) from JSPS.

- 1) K. Ishida, Y. Nakai, and H. Hosono, J. Phys. Soc. Jpn. **78**, 062001 (2009).
- 2) J. Paglione and R. L. Greene, Nat. Phys. **6**, 645 (2010).
- 3) D. C. Johnston, Adv. Phys. **59**, 803 (2010).
- 4) Y. Kamihara, T. Watanabe, M. Hirano, and H. Hosono, J. Am. Chem. Soc. **130**, 3296 (2008).
- 5) M. Rotter, M. Tegel, and D. Johrendt, Phys. Rev. Lett. **101**, 107006

- (2008).
- 6) K. Kudo, K. Iba, M. Takasuga, Y. Kitahama, J. Matsumura, M. Danura, Y. Nogami, and M. Nohara, Sci. Rep. **3**, 1478 (2013).
- 7) J. H. Tapp, Z. Tang, B. Lv, K. Sasmal, B. Lorenz, P. C. W. Chu, and A. M. Guloy, Phys. Rev. B **78**, 060505(R) (2008).
- 8) F.-C. Hsu, J.-Y. Luo, K.-W. Yeh, T.-K. Chen, T.-W. Huang, P. M. Wu, Y.-C. Lee, Y.-L. Huang, Y.-Y. Chu, D.-C. Yan, and M.-K. Wu, Proc. Natl. Acad. Sci. U.S.A. **105**, 14262 (2008).
- 9) N. Kawaguchi, H. Ogino, Y. Shimizu, K. Kishio, and J. Shimoyama, Appl. Phys. Express **3**, 063102 (2010).
- 10) X. Zhu, F. Han, G. Mu, P. Cheng, B. Shen, B. Zeng, and H.-H. Wen, Phys. Rev. B **79**, 220512(R) (2009).
- 11) H. Ogino, K. Machida, A. Yamamoto, K. Kishio, J. Shimoyama, T. Tohei, and Y. Ikuhara, Supercond. Sci. Technol. **23**, 115005 (2010).
- 12) P. M. Shirage, K. Kihou, C.-H. Lee, H. Kito, H. Eisaki, and A. Iyo, Appl. Phys. Lett. **97**, 172506 (2010).
- 13) S. Kakiya, K. Kudo, Y. Nishikubo, K. Oku, E. Nishibori, H. Sawa, T. Yamamoto, T. Nozaka, and M. Nohara, J. Phys. Soc. Jpn. **80**, 093704 (2011).
- 14) M. Nohara, S. Kakiya, K. Kudo, Y. Oshiro, S. Araki, T. C. Kobayashi, K. Oku, E. Nishibori, and H. Sawa, Solid State Commun. **152**, 635 (2012).
- 15) N. Ni, J. M. Allred, B. C. Chan, and R. J. Cava, Proc. Natl. Acad. Sci. **108**, E1019 (2011).
- 16) C. Löhnert, T. Stürzer, M. Tegel, R. Frankovsky, G. Friederichs, and D. Johrendt, Angew. Chem. Int. Ed. **50**, 9195 (2011).
- 17) C. Hieke, J. Lippmann, T. Stürzer, G. Friederichs, F. Nitsche, F. Winter, R. Pöttgen, and D. Johrendt, Phil. Mag. **93**, 3680 (2013).
- 18) K. Kudo, D. Mitsuoka, M. Takasuga, Y. Sugiyama, K. Sugawara, N. Katayama, H. Sawa, H. S. Kubo, K. Takamori, M. Ichioka, T. Fujii, T. Mizokawa, and M. Nohara, Sci. Rep. **3**, 3101 (2013).
- 19) Z.-A. Ren, W. Lu, J. Yang, W. Yi, X.-L. Shen, Z.-C. Li, G.-C. Che, X.-L. Dong, L.-L. Sun, F. Zhou, and Z.-X. Zhao, Chin. Phys. Lett. **25**, 2215 (2008).
- 20) N. Katayama, K. Kudo, S. Onari, T. Mizukami, K. Sugawara, Y. Sugiyama, Y. Kitahama, K. Iba, K. Fujimura, N. Nishimoto, M. Nohara, and H. Sawa, J. Phys. Soc. Jpn. **82**, 123702 (2013).
- 21) H. Yakita, H. Ogino, T. Okada, A. Yamamoto, K. Kishio, T. Tohei, Y. Ikuhara, Y. Gotoh, H. Fujihisa, K. Kataoka, H. Eisaki, and J. Shimoyama, J. Am. Chem. Soc. **136**, 846 (2014).
- 22) A. Sala, H. Yakita, H. Ogino, T. Okada, A. Yamamoto, K. Kishio, S. Ishida, A. Iyo, H. Eisaki, M. Fujioka, Y. Takano, M. Putti, and J. Shimoyama, Appl. Phys. Express **7**, 073102 (2014).
- 23) D. Rutzinger, C. Bartsch, M. Doerr, H. Rosner, V. Neu, Th. Doert, and M. Ruck, J. Solid State Chem. **183**, 510 (2010).
- 24) K. Kudo, T. Mizukami, Y. Kitahama, D. Mitsuoka, K. Iba, K. Fujimura, N. Nishimoto, Y. Hiraoka, and M. Nohara, J. Phys. Soc. Jpn. **83**, 025001 (2014).
- 25) C.-H. Lee, A. Iyo, H. Eisaki, H. Kito, M. T. Fernandez-Diaz, T. Ito, K. Kihou, H. Matsuhata, M. Braden, and K. Yamada, J. Phys. Soc. Jpn. **77**, 083704 (2008).
- 26) H. Usui and K. Kuroki, Phys. Rev. B **84**, 024505 (2011).
- 27) K. Kuroki, H. Usui, S. Onari, R. Arita, and H. Aoki, Phys. Rev. B **79**, 224511 (2009).
- 28) Y. Mizuguchi, Y. Hara, K. Deguchi, S. Tsuda, T. Yamaguchi, K. Takeda, H. Kotegawa, H. Tou, and Y. Takano: Supercond. Sci. Technol. **23**, 054013 (2010).
- 29) By doping P in a range of more than 1%, the La doped 112 phase was not obtained.
- 30) The values of  $\alpha$  and  $h_{Pn}$  were determined on the basis of the crystal structure with the space group  $P2_1$  proposed by Katayama *et al.*<sup>20</sup> We have checked that they are nearly unchanged even when using the space group  $P2_1/m$  proposed by Yakita *et al.*<sup>21</sup>
- 31) The increased  $a$  parameter [Fig. 4(a)] results in an increased  $\alpha_a$ , but the nearly ideal condition of  $\alpha_a$  in the Sb-free sample remains almost unchanged in the Sb-doped sample.